Application of spatially resolved thermoreflectance for the study of facet heating in high power semiconductor lasers

MACIEJ BUGAJSKI[*], TOMASZ OCHALSKI, TOMASZ PIWOŃSKI, DOROTA WAWER

Institute of Electron Technology, al. Lotników 32/46, 02 668 Warsaw, Poland

[*]Corresponding author: M. Bugajski, bugajski@ite.waw.pl

We have developed a new technique for monitoring the facet heating in semiconductor lasers and for correlating these measurements with the performance and reliability of the device. The method is based on thermoreflectance, which is a modulation technique relying on periodic facet temperature modulation induced by pulsed current supply of the laser. The periodic temperature change of the laser induces variation of the refractive index and consequently modulates the probe beam reflectivity. The technique has a spatial resolution of about 1 μm and temperature resolution better than 1 K, and can be used for temperature mapping over a 300 μm × 300 μm area. It can be applied to any kind of edge emitting lasers or laser bars. The technique is crucial for understanding the thermal behavior of a device.

Keywords: thermoreflectance, semiconductor lasers.

1. Introduction

The temperature at the facet has a critical role in the performance and reliability of a device. Catastrophic optical damage (COD) failure of a laser device occurs at the facet and is caused by absorption of light at the facet, which leads to a local band-gap reduction with consequent increased absorption and temperature rise. The runaway effect leads to failure of the device. Thus the local temperature of the facet is indicative of these processes. In addition, the lateral temperature profile creates a refractive index profile which has a strong effect on device performance. The lateral refractive index profile induced by a non-uniform junction heating plays a dominant role in determining lateral modes and emission characteristics of broad-area lasers during continuous (CW) and long-pulse operation. This is due to thermal focusing caused by temperature induced lateral index profile. Understanding and characterizing these thermal effects is important to the development of high power CW lasers. The measurements also qualify the bonding quality and optimum choice of substrate material for heat removal.

2. Spatially-resolved thermoreflectance (TR) system.

2.1. Basic concepts and experimental set-up

Optical modulation spectroscopy techniques are designed to measure the response of the optical constants of a solid to a periodic change of an applied perturbation. Thermoreflectance (TR), which is used here as a method of determining local absolute temperature of the semiconductor laser mirror, relies on periodic facet temperature modulation induced by pulsed current supply of the laser. The method was introduced by EPPERLAIN [1, 2] and further developed by HAYAKAWA [3] and SCHAUB [4]. This work concentrates on the improvement of spatial resolution and exploration of mapping possibilities of this technique. We also analyze the usefulness of thermoreflectance for monitoring fabrication technology of semiconductor lasers.

The periodic temperature change of the laser induces variations of the dielectric function $\varepsilon(E) = \varepsilon_1(E) + \varepsilon_2(E)$, and consequently, modulates the probe beam reflectivity

$$\frac{\Delta R}{R} = \alpha \Delta \varepsilon_1 + \beta \Delta \varepsilon_2 \tag{1}$$

In thermoreflectance, these variations are brought about by the temperature dependence of the bandgap E_g and temperature dependence of the broadening parameter Γ,

$$\Delta \varepsilon = \frac{\partial \varepsilon}{\partial T} \Delta T = \frac{\partial \varepsilon}{\partial E_g} \frac{\mathrm{d} E_g}{\mathrm{d} T} \Delta T + \frac{\partial \varepsilon}{\partial \Gamma} \frac{\mathrm{d} \Gamma}{\mathrm{d} T} \Delta T \tag{2}$$

The contribution of the last mechanism is usually negligible, and in that sense, thermoreflectance is basically a bandgap modulation technique. As a result, the relative variation of sample reflectance $\Delta R/R$ is linear as a function of the temperature variation ΔT, and measurement of sample reflectance allows us to determine an increase of the local temperature from a simple formula:

$$\Delta T = \left(\frac{1}{R} \frac{\partial R}{\partial T} \right)^{-1} \frac{\Delta R}{R} \equiv \kappa \frac{\Delta R}{R} \tag{3}$$

The thermoreflectance calibration coefficient κ depends on: the material [5], the specific details of the experimental set-up (numerical aperture of the microscope objective) [6], and most importantly, the wavelength of probe light [7].

The devices for the measurements are mounted on a high precision *x-y-z* translator stage to align laser mirror to the probe laser beam which is reflected from the facet. The probe beam spot size is diffraction limited and can be as low as 1 μm. The beam spot and the laser facet are observed with CCD video camera and displayed at the CRT monitor under high magnification, which allows accurate probing of specific regions of the laser. Using piezoelectrically driven translator stages makes it possible to obtain

maps of the temperature distribution over the laser facet. The lasers are typically supplied with low frequency pulsed current (50–200 Hz) with filling factor 10–50%. Under these conditions the laser is operating quasi-CW and is subjected to the thermal effects associated with CW operation. The periodic temperature change of the laser induces variations of the refractive index and consequently modulates the probe beam reflectivity.

Figure 1 shows the experimental set-up developed for the thermoreflectance measurements of facet heating in semiconductor lasers. The temperature induced changes of the probe beam reflectivity are generally small ($\sim 10^{-5}$ K^{-1}) and depend on the probe beam wavelength. We limit ourselves to single wavelength measurements and perform the mapping of temperature distribution, using calibration described in the subsequent section. The spatial resolution of the system is determined by: i) probe beam focusing and ii) positioning accuracy of translation stages. The probe beam can be focused, using special techniques, down to a single micron diameter.
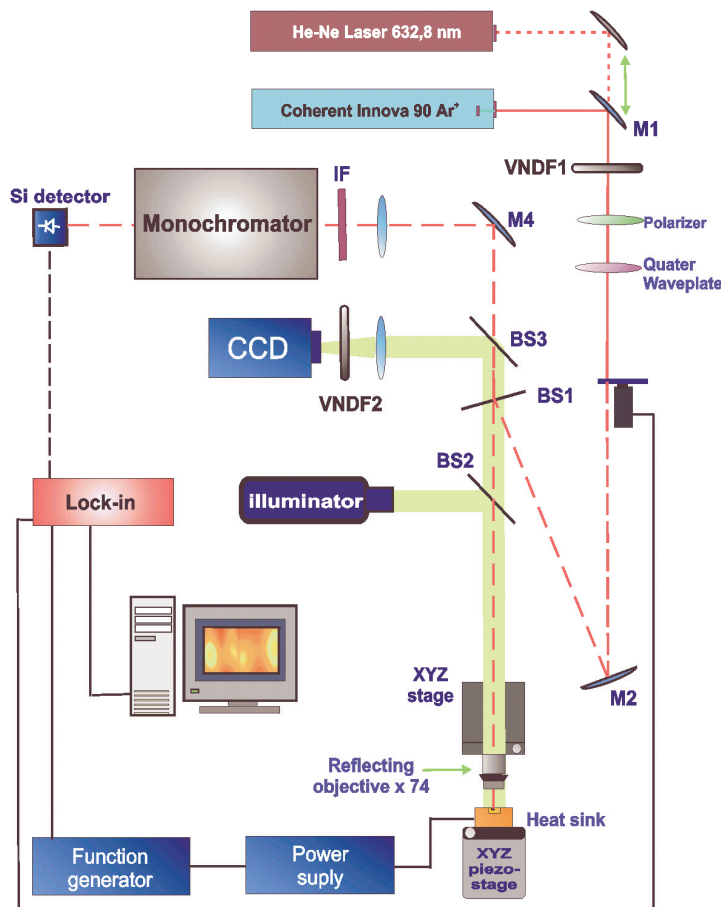

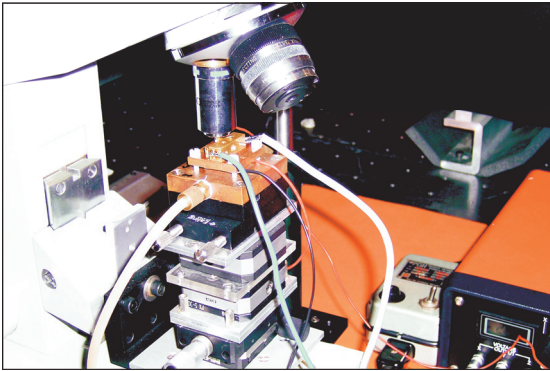Fig. 1. Experimental set-up for thermoreflectance mapping of laser facets.

Fig. 2. Experimental set-up for thermoreflectance mapping of laser facets (details of focusing head and piezoelectric translation stages).

The piezoelectric transducers allow a 300×300 µm^2 scanning range with 0.2 µm positioning accuracy. The vertical positioning is also done by piezoelectric transducer. The positioning of the laser facet in the focal plane of the optical system is crucial for focusing. The probe beam focusing on the sample is done with reflecting microscope objective. Because of its all reflecting construction it is free from chromatic aberration. The objective consists of a small convex primary mirror and a larger concave secondary mirror. The experiments showed that the reflecting objective has clear advantages over refracting optics of equivalent aperture and focal length. The software for controlling the movement of *x-y-z* microstages and data acquisition uses the Lab View platform. The movement of the piezoelectric stages is controlled by IEEE interface. A photograph showing details of the experimental set-up, *i.e.*, piezoelectric positioning system and focusing optics (reflecting microscope objective) is presented in Fig. 2.

2.2. Temperature calibration

The accurate calibration method is an essential element of any quantitative thermometry techniques. This is of particular importance for the thermoreflectance studies of semiconductor lasers, whose constituent materials have optical properties that are not well-characterized or can vary depending on the processing details. The data avaible for the absolute values of thermoreflectance coefficient κ is very scarce. Reported values of the facet temperature under high power operation scatter in the wide range, although each measuring technique is based on the temperature dependence of inherent material parameters, such as refractive index and energy gap. Therefore, the absolute facet temperatures reported are difficult to compare. Due to the fact that the coefficient κ depends on both the material probed and the experimental conditions, it should not be taken from the literature, but rather determined *in-situ*, on the probed material itself. In our method, the temperature of a sample is controlled externally while variations in its reflectance are measured. The advantage of this approach lies in a relatively
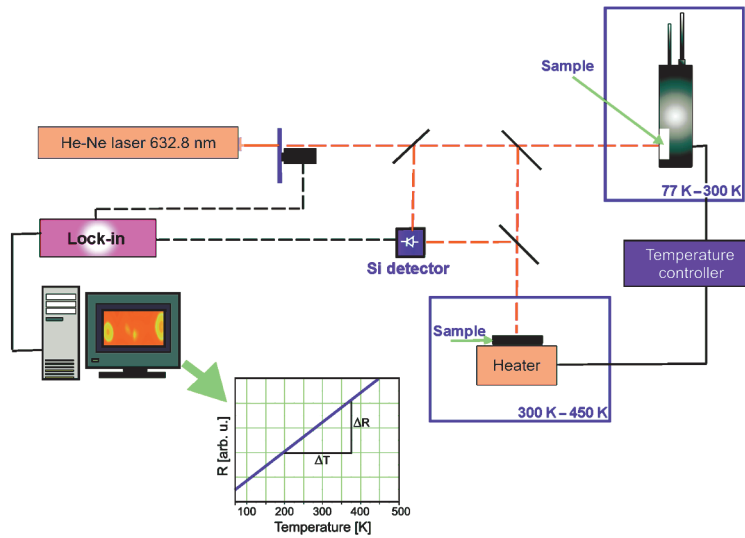
Fig. 3. Experimental set-up for determination of thermoreflectance coefficient.

simple experimental set-up and measuring procedure. However, this method is difficult to apply to optical systems with a large numerical aperture and a shallow focal depth, which are needed to achieve high spatial resolution, because thermal expansion of a sample–heater assembly can lead to errors. This problem can be avoided by preparing a dedicated calibration sample with a large surface area assuring uniform temperature distribution and by using a separate optical system for calibration with a larger diameter of the probe beam spot.

The thermoreflectance coefficient has been determined in a special experimental arrangement shown in Fig. 3. The calibration process relied on the measurement of reflectance coefficient R for the range of specific values of temperature T. Since the variations of reflectance coefficient are relatively small the calibration has to be done in broad temperature range (in our case 77–500 K; the corresponding change of reflectivity is of the order of $10^{-3}R$). The temperature range 77–300 K has been attained by using variable temperature liquid nitrogen cryostat. The temperatures above 300 K were attained by using resistance heaters. The temperature has been measured with 0.1 K accuracy. The calibration has been done for the probe beam wavelength 632.8 nm (He-Ne laser) and normal incidence as it is the wavelength most frequently used for measurements. The reflected beam intensity was measured by silicon photodiode. The GaAs substrate material (n-type, 2×10^{18} cm^{-3}) has been used for calibration as it constitutes majority of the facet. The other materials composing laser structure (InGaAs, AlGaAs) are assumed for the moment to have the same thermoreflectance coefficient. The GaAs wafer of the size 10 mm×10 mm was used to assure uniform temperature distribution over the surface which is important

for accurate temperature determination during measurements. The value of thermo-reflectance coefficient κ has been determined from Eq. (3). For the probe beam wavelength $\lambda = 632.8$ nm it has been estimated for 8.0×10^3 K.

The value of thermoreflectance constant has been further verified by microphoto-luminescence measurements performed in essentially the same experimental set-up that used for as thermoreflectance measurements. Photoluminescence measurements performed on operating lasers offer the possibility of determining the temperature changes of the facet from the shift of the PL peak referring to band-to-band transitions in the material. As it is commonly accepted in [9, 10], when assuming that at temperatures around 300 K, PL peak in GaAs shifts with temperature by 0.3 nm/K, it was possible to determine the laser facet temperature at any specific point. The spatial resolution
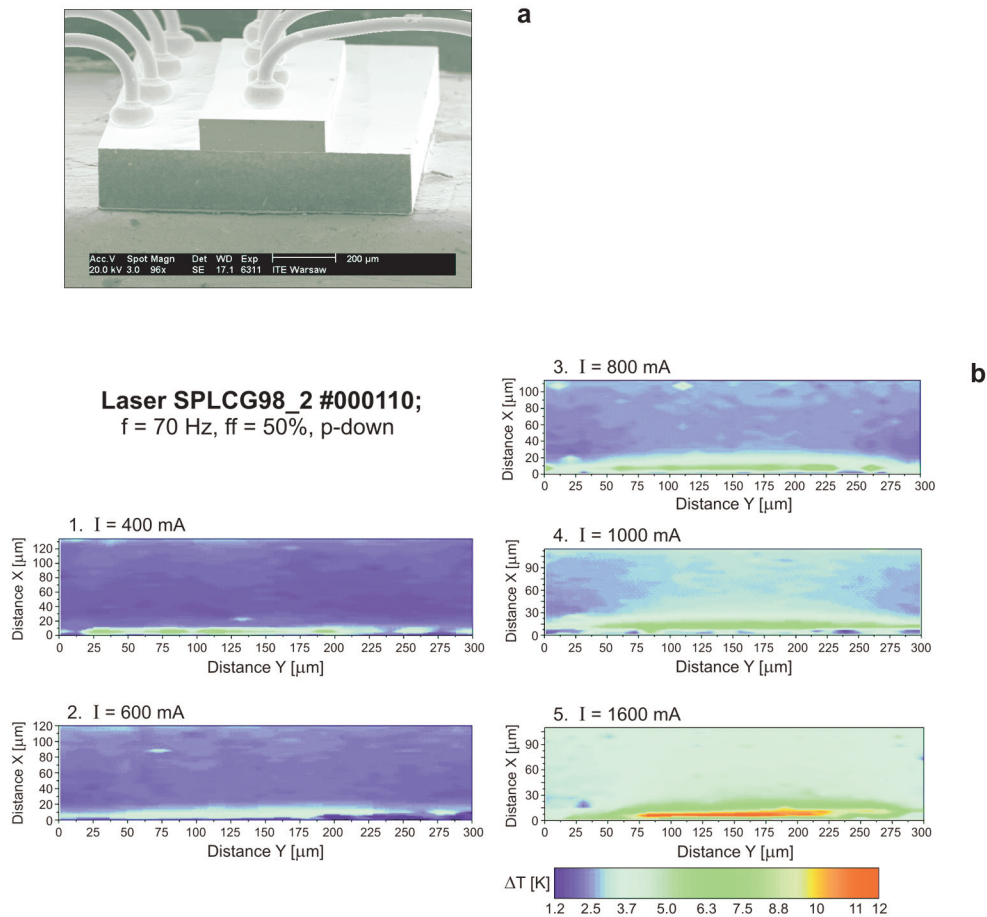

Fig. 4. SEM picture of the reference laser emitting at $\lambda = 980$ (*p*-down mounted on SiC submount and soldered to copper heat sink) – **a**. The facet temperature maps for the investigated laser under investigation for different supply currents (the CW optical power emitted for each supply current equals: 50, 250, 450, 650 and 1300 mW, respectively) – **b**.

of micro-photoluminescence is comparable to that of thermoreflectance since both methods use the same optical set-up for focusing the PL exciting beam. The results of micro-photoluminescence confirm the earlier determined value of thermoreflectance coefficient. The calibration can also be done by micro-Raman (μ-R) measurements. The last method offers more straightforward temperature determination (from the intensity ratio of anti-Stokes and Stokes lines) than photoluminescence, but is much more complicated from the experimental point of view [11–13].

3. Experimental study of facet heating in high power semiconductor lasers

In the following we will compare the performance of lasers mounted *p*-side down and *p*-side up on different heat sinks. The devices with cleaved facets will be analyzed. The reference device to start with is InGaAs/GaAs laser emitting at λ = 980 nm, and shown in Fig. 4**a**. The laser has a cleaved facet Fabry–Perot resonator and is *p*-down soldered onto SiC submount and copper heat sink. The facets are coated with AR/HR coatings. The laser shows superior thermal properties and emits CW up to 2.5 W. The temperature distribution maps for the front output facet recorded at different values
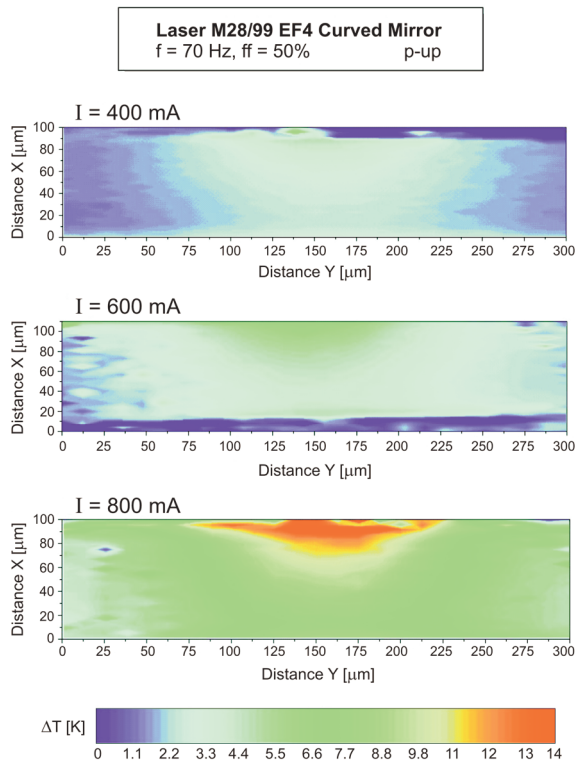

Fig. 5. Facet temperature maps for *p*-up mounted laser for two different supply currents.

of drive current are shown in Fig. 4**b**. Heating is practically limited to the active region and junction temperatures are in low teens, even for currents well above 1 A. The above results are compared with an example of *p*-up mounted device soldered directly to the copper heat sink. The junction temperatures are slightly higher than in the previous case due to less efficient heat extraction in the case of *p*-side up mounting (see Fig. 5). By numerical analysis of temperature data one can construct the map of heat flux distribution in the cross-section of the device. The heat flux magnitude is assumed to be proportional to the temperature gradient in particular direction. The result is shown in Fig. 6, where it is compared with calculated heat flux distribution. A vectorial type
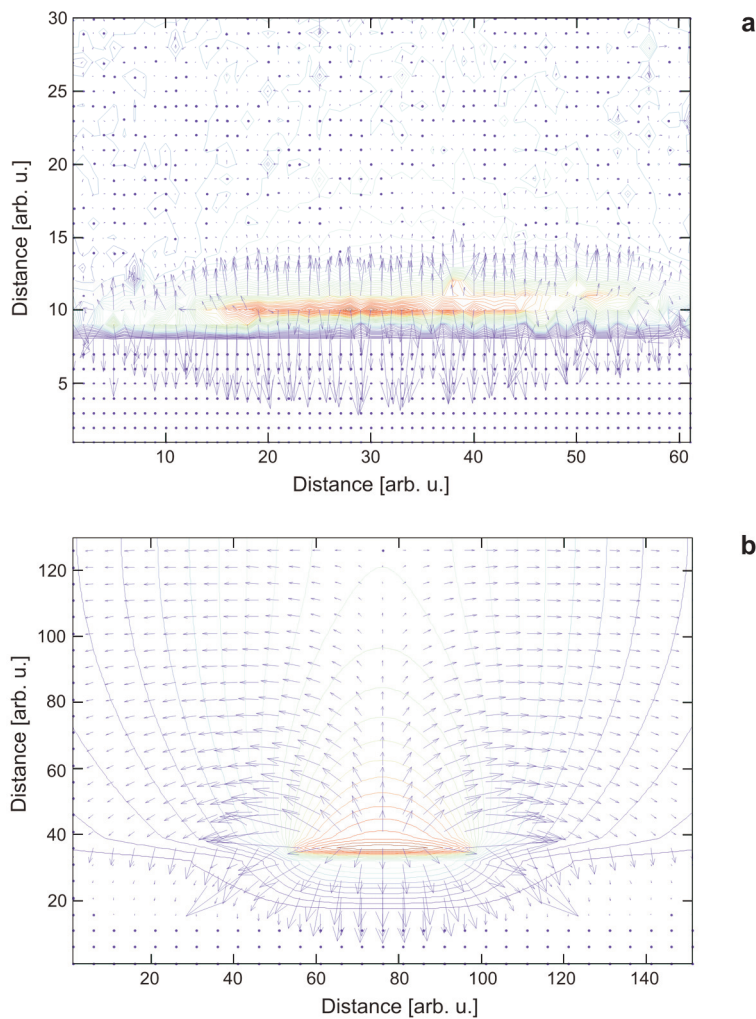

Fig. 6. Heat flux distribution in *p*-down mounted laser; experimental – **a**, calculated – **b**. The magnitude of each arrow represents the value of the flux and the orientation of the arrow shows the flux spatial direction.

Fig. 8. Example of facet temperature map and reflectivity map for CIBE etched laser. SEM picture of the facet is also shown.
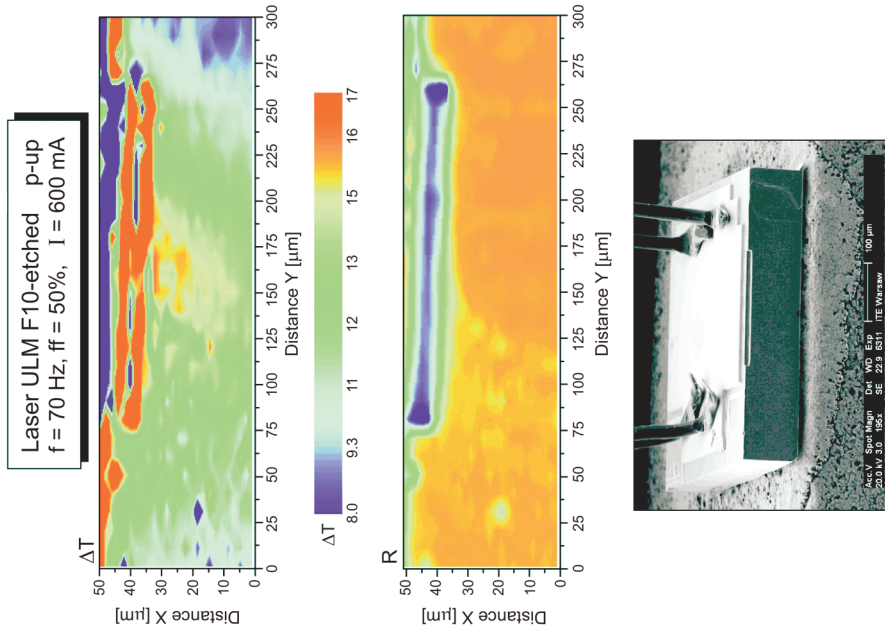

Fig. 7. Example of facet temperature map and corresponding reflectivity map for the laser exposed to oxygen plasma (RIE process). SEM picture of the facet is also shown.
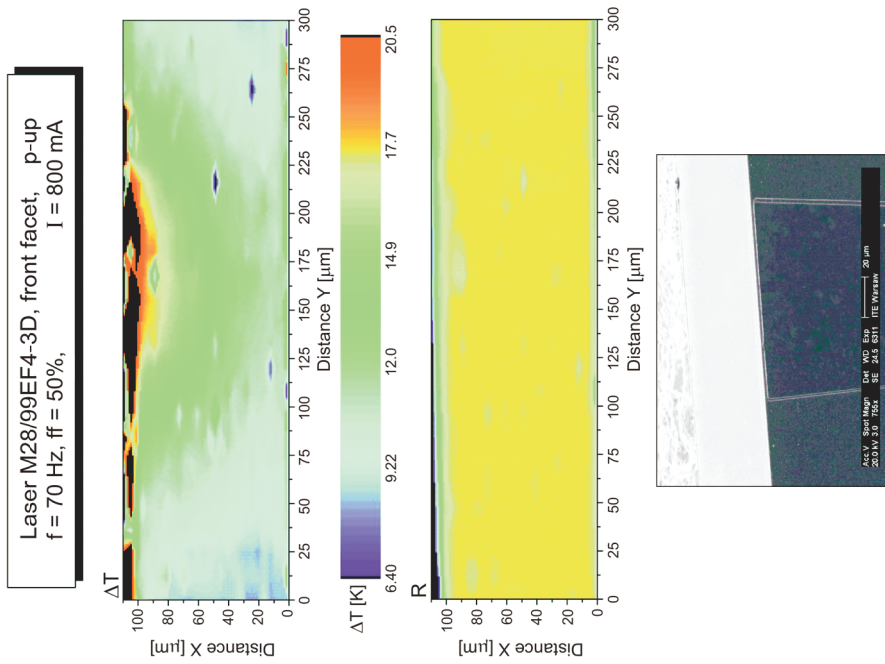
of diagram has been chosen as best illustrating the data discussed. It can be seen that in *p*-down mounted devices, heat generated in the active region is effectively extracted to the heat sink, although an upward heat transfer through the substrate cannot be neglected. This kind of analysis can be particularly useful when dealing with the heat transport in the devices with complicated geometry.

We have also evaluated facet damage caused by different ion beam etching techniques used to produce curved mirrors in unstable resonator geometry. The actual accuracy of temperature mapping on curved mirrors depends on the mirror radius and is generally lower than in the case of flat mirrors. This is due to the probe beam defocusing effects. To minimize this problem one has to either sacrifice high spatial resolution of the measurements or to relay on special test lasers. To get the best possible results we have decided to choose the second approach. Special test lasers with plane parallel cleaved and etched mirrors were fabricated for thermoreflectance measurements. The devices under study fall into two groups. The first group of lasers (1F and 3D) are *p*-up mounted, 1 mm long devices with the back mirror curvature of 300 µm and magnification $M = 11$. The laser 1F has cleaved front facet, 3D is all the same except being additionally exposed to oxygen plasma to simulate the damage created by curved mirror fabrication. The F7 and F 10 devices are cleaved and CIBE etched, respectively.

The temperature distribution maps for oxygen plasma RIE etched laser and CIBE etched laser are shown in Figs. 7 and 8. No excessive damage to the mirror surface, produced by etching, is observed. The temperature increase above the ambient temperature at the facet is slightly higher for oxygen plasma treated surfaces (about 20 K for 600 mA), compared to 17 K for CIBE etched surfaces. It is 1.5–2 times higher than for cleaved surfaces. The fact that neither for RIE nor for CIBE we observe excessive heating of the surface is clear evidence that both etching techniques can be used for mirror shaping; at least so far as thermal parameters of the lasers are concerned.

4. Conclusions

In this paper, we have used spatially resolved thermoreflectance to measure temperature distribution over the facet of high power semiconductor lasers. The technique has a spatial resolution of about 1 µm and temperature resolution better than 1 K. Despite the necessity of being calibrated by the other independent method, like for example, band-to-band photoluminescence, thermoreflectance has one major advantage over µ-PL and µ-R spectroscopy – it allows a high resolution mapping of temperature distribution over large areas (300 µm×300 µm), which is otherwise difficult and time consuming. Thermal management problems are still not completely solved in high power lasers and appear to be a limiting factor in exploitation of their full industrial potential. Therefore direct methods of probing temperature distribution in the devices

are very important for the optimization of their construction and evaluation of both different mounting techniques as well as passivation and etching methods.

References

[1] EPPERLEIN P.W., *Micro-temperature measurements on semiconductor laser mirrors by reflectance modulation: A newly developed technique for laser characterization*, Japanese Journal of Applied Physics, Part 1: Regular Papers and Short Notes **32**(12A), 1993, pp. 5514–22.

[2] EPPERLEIN P.W., BONA G.L., *Influence of the vertical structure on the mirror facet temperatures of visible GaInP quantum well lasers*, Applied Physics Letters **62**(24), 1993, pp. 3074–6.

[3] HAYAKAWA T., *Facet temperature distribution in broad stripe high power laser diodes*, Applied Physics Letters **75**(10), 1999, pp. 1467–9.

[4] SCHAUB E., *Optical absorption rate determination, on the front facet of high-power GaAs laser diodes, by means of thermoreflectance technique*, Japanese Journal of Applied Physics, Part 1: Regular Papers, Short Notes and Review Papers **40**(4B), 2001, pp. 2752–6.

[5] MATATAGUI E., THOMPSON A.G., CARDONA M., *Thermoreflectance in semiconductors*, Physical Review **176**(3), 1968, pp. 950–60.

[6] DILHAIRE S., GRAUBY S., CLAEYS W., *Calibration procedure for temperature measurements by thermoreflectance under high magnification conditions*, Applied Physics Letters **84**(5), 2004, pp. 822–4.

[7] TESSIER G., HOLE S., FOURNIER D., *Quantitative thermal imaging by synchronuous thermoreflectance with optimized illumination wavelengths*, Applied Physics Letters **78**(16), 2001, pp. 2267–9.

[8] OZAKI S., ADACHI S., *Spectroscopic ellipsometry and thermoreflectance of GaAs*, Journal of Applied Physics **78**(5), 1995, pp. 3380–6.

[9] HALL D.C., GOLDBERG L., MEHUYS D., *Technique for lateral temperature profiling in optoelectronic devices using a photoluminescence microprobe*, Applied Physics Letters **61**(4), 1992, pp. 384–6.

[10] ROMMEL J.M., GAVRILOVIC P., DABKOWSKI F.P., *Photoluminescence measurement of facet temperature of 1 W gain-guided AlGaAs/GaAs laser diodes*, Journal of Applied Physics **80**(11), 1996, pp. 6547–9.

[11] EPPERLEIN P.W., BONA G.L., ROENTGEN P., *Local mirror temperatures of red-emitting (Al)GaInP quantum-well laser diodes by Raman scattering and reflectance modulation measurements*, Applied Physics Letters **60**(6), 1992, pp. 680–2.

[12] PUCHERT R., BARWOLFF A., MENZEL U., LAU A., VOSS M., ELSAESSER T., *Facet and bulk heating of GaAs/AlGaAs high-power laser arrays studied in spatially resolved emission and micro-Raman experiments*, Journal of Applied Physics **80**(10), 1996, pp. 5559–63.

[13] TOMM J.W., THAMM E., BARWOLFF A., ESAESSER T., LUFT J., BAEUMLER M., MUELLER S., JANTZ W., RECHENBERG I., ERBERT G., *Facet degradation of high-power diode laser arrays*, Applied Physics A: Materials Science Processing **A70**(4), 2000, pp. 377–81.